Interaction of lipoprotein lipase with homogeneous lipid emulsions

Cait E. MacPhee,* Robert Y. S. Chan,* William H. Sawyer,* Walter F. Stafford,† and Geoffrey J. Howlett[1,]*

Russell Grimwade School of Biochemistry and Molecular Biology,* University of Melbourne, Parkville, Victoria 3052, Australia, and Boston Biomedical Research Institute,† Boston, MA 02114-2500

Abstract The central function of lipoprotein lipase (LpL) is to hydrolyze triacylglycerols in chylomicrons and very low density lipoproteins. We have examined the binding of purified milk lipoprotein lipase to homogeneous synthetic lipid emulsions. Emulsions composed of either naturally occurring ester-linked lipids or the non-hydrolyzable ether analogues were prepared by sonication and pressure extrusion, and fractionated by sucrose density gradient centrifugation. Flotation analysis using the analytical ultracentrifuge indicated that the individual fractions were relatively homogeneous with respect to size with flotation coefficients and molecular weights for the separated fractions ranging from 100 to 1100 S and 5.2×10^7 to 6.0×10^8, respectively. Purified milk lipoprotein lipase bound with high affinity and in a saturable manner to emulsions prepared from the non-hydrolyzable ether-linked lipid analogues of 1-oleoyl, 2-palmitoyl phosphatidylcholine and triolein. At low concentrations of LpL, the enzyme caused aggregation of the emulsion particles by interparticle cross-linking. At higher LpL concentrations, the flotation coefficient of the emulsions decreased significantly with a concomitant increase in particle density. At saturation, the number of LpL monomers bound to lipid particles of radii 67, 75, and 79 nm was 1315, 1449, and 1466, respectively. The results demonstrate close packing of LpL on the lipid surface and are consistent with there being little disruption to the overall structure of the emulsion particle.—**MacPhee, C. E., R. Y. S. Chan, W. H. Sawyer, W. F. Stafford, and G. J. Howlett.** Interaction of lipoprotein lipase with homogeneous lipid emulsions. *J. Lipid Res.* 1997. **38:** 1649–1659.

Supplementary key words ether-linked lipids • sedimentation velocity • sedimentation equilibrium • protein–lipid interactions • flotation velocity • lipid monolayer

Lipoprotein lipase (LpL) hydrolyzes triacylglycerol (TG), phosphatidylcholine (PC), and diacylglycerol in TG-rich very low density lipoprotein particles (VLDL) and chylomicrons (for review see ref. 1). These particles consist predominantly of a TG and cholesteryl ester core surrounded by a monolayer of phospholipids, protein, and unesterified cholesterol (2). Active dimeric LpL (3) is bound to the endothelial cell surface by interaction via glycosaminoglycans (4). LpL-catalyzed hydrolysis of lipid near the cell surface plays an important role in the metabolism of triacylglycerol-rich lipoproteins. An additional non-enzymatic role has been proposed where LpL binds cholesterol-rich lipoproteins and lipoprotein remnants and mediates cellular uptake and degradation via interaction with specific protein receptors on the cell surface (5–8).

Changes to the structure of lipoproteins in vivo require the interaction of a number of proteins (enzymes and lipid transfer proteins) with the surface of the lipoprotein particle. Examination of the mechanisms and the specificity of these interactions requires model lipid surfaces of defined structure and composition. A number of such models have been developed to examine the events involved in the binding of LpL to lipid surfaces. Studies with lipid monolayers show that LpL has a higher affinity for monolayers containing long chain unsaturated triacylglycerols (9, 10), and that increases in surface pressure eventually lead to a decline in enzyme activity (11). Spherical lipid emulsions composed of a surface monolayer of phospholipid enclosing a core of triacylglycerol more closely resemble the lipid structure of natural lipoproteins (12–15). Using emulsions the size of either low density lipoprotein (LDL) or chylomicrons, Tajima, Yokoyama, and Yamamoto (16) showed that the kinetics of triacylglycerol hydrolysis were similar with respect to K_m but that V_{max} was greater for the chylomicron-sized particles. More recently Connelly et al. (17) reported that the K_m was lower for small native VLDL particles than for large ones, but that V_{max}

Abbreviations: LpL, lipoprotein lipase; TG, triacylglycerol; PC, phosphatidylcholine; VLDL, very low density lipoprotein particles; DMPC, ester-linked dimyristoyl phosphatidylcholine (1,2-ditetradecanoyl-*sn*-glycero-3-phosphocholine); OPPC, ether-linked 1-oleoyl,2-palmitoyl phosphatidylcholine (1-O-hexadecyl-2-[(*cis*)-9-octadecanoyl]-rac-glycero-3-phosphocholine); TO, triolein (1,2,3-tri[*cis*-9-octadecanoyl]glycerol).

[1]To whom correspondence should be addressed.

values were similar. Both studies involved populations of particles that were relatively heterogeneous with respect to size and composition (18, 19). Such studies highlight the need for a model system consisting of well-characterized emulsion particles of homogeneous size and composition.

The binding of LpL to lipid surfaces must be studied in the absence of the hydrolytic reaction that might otherwise perturb the binding equilibrium. Ether-linked phospholipids have been used previously to study the interaction of LpL with phospholipid vesicles (20). The physical properties of ether phospholipid analogues are similar to those of the native molecule with respect to transition temperature, bilayer vesicle stability, and the binding of apolipoproteins (21). Moreover, the ability of LpL to hydrolyze triacylglycerol solubilized in an ether–phospholipid monolayer is comparable to its activity against triacylglycerol solubilized in the ester lipid (10). The present study describes a new approach to the preparation of synthetic lipid emulsions that generates a series of relatively homogeneous emulsion fractions of defined size. Such populations have potential value in studies of the effect of particle size on the binding of proteins to specific lipid surfaces. We have used size-fractionated emulsions composed of non-hydrolyzable ether-linked analogues of both PC and TG to investigate the hydrodynamic properties of LpL–lipid emulsion complexes and to characterize the binding of LpL to spherical lipid surfaces.

MATERIALS AND METHODS

Materials

Ester-linked dimyristoyl phosphatidylcholine (1,2-ditetradecanoyl-*sn*-glycero-3-phosphocholine, DMPC) and ether linked 1-oleoyl,2-palmitoyl phosphatidylcholine (1-O-hexadecyl-2-[(*cis*)-9-octadecanoyl]-rac-glycero-3-phosphocholine, OPPC) were purchased from Sigma, St. Louis, MO. Triolein (1,2,3-tri[*cis*-9-octadecanoyl]glycerol, TO) was purchased from Nu-Chek Prep, Elysian, MN. Porcine intestinal mucosa heparin (sodium salt) was purchased from Sigma. Ether-linked triolein was prepared by azeotropic distillation according to the procedure of Halperin, Stein, and Stein (22).

Emulsion preparation

Emulsions were prepared with an initial ratio of triacylglycerol:phosphatidylcholine of 2:1. Lipids were dried under a stream of nitrogen and left under vacuum overnight to remove any traces of organic solvent, and resuspended in 0.1 M potassium phosphate buffer, pH 7.4. Final lipid concentrations were 1.5 mg/ml in a total volume of 10 ml. The suspension was sonicated at maximum power (amplitude 165 microns) in an MSE Soniprep sonicator (5 × 1 min with 30 s intervals for cooling) under a constant stream of nitrogen. The temperature of the jacketed vial was maintained at 34°C with a circulating water bath. The dispersion was extruded 11 times through two polycarbonate 100-nm filters using a LiposoFast hand-held microextruder (Avestin Inc., Ottawa, ONT). After extrusion, the density of the extrudate was increased to 1.038 g/ml by the addition of solid sucrose (10 g/dL) and the sample was layered beneath 0.1 M potassium phosphate buffer (pH 7.4) in heat-sealable polycarbonate centrifuge tubes (Beckman) to form a discontinuous sucrose gradient. This sample was centrifuged at 40,000 rpm for 35 min in the 70.1 Ti rotor of a Beckman model L8-70 preparative ultracentrifuge (110,000 *g*) to separate emulsion particles from phospholipid vesicles which remain at the sucrose-buffer interface. After centrifugation, the top 1.0 ml of the tube was taken and the density was increased to 1.018 g/ml with solid sucrose (5 g/dL) before layering beneath a preformed 0–5% (w/v) linear sucrose gradient prepared in 0.1 M phosphate buffer, pH 7.4. Tubes were centrifuged at 6000 rpm in the SW-40 rotor of a Beckman model L8-70 preparative ultracentrifuge for 2 h (4500 *g*). These centrifugation conditions were chosen from simulations of the centrifugal behavior of spherical particles of molecular weight 1.7×10^8 and radius 42 nm using the program SIMCENT (kindly provided by Dr. A. P. Minton, National Institutes for Health, Bethesda, MD). The linearity and stability of the sucrose gradients, with and without the emulsion preparation, was established by fractionation and colorimetric analysis of a 0–0.5 mg/ml bromphenol blue gradient formed concurrently with the sucrose gradient (results not shown). Fractions (1.0 ml) for analysis were collected from the bottom of the tubes. Fractions were dialyzed against 0.1 M potassium phosphate, pH 7.4, to remove sucrose prior to centrifugation studies or against water prior to phospholipid analysis. Phospholipid concentrations were determined by phosphate estimation using a modified Allen method (23). Triacylglycerol concentrations were determined using a lipase assay kit (Boehringer Mannheim, Australia). Absorption spectra were measured using a Cary 5 spectrophotometer (Varian, Australia) and were analyzed to obtain the average particle diameter (D) using equation [2] of Easterbrook-Smith (24) where D is comparable to, but less than, the wavelength of light (25).

Isolation of lipoprotein lipase

Lipoprotein lipase was isolated from bovine milk by heparin-agarose affinity chromatography as described

by Bengtsson-Olivecrona and Olivecrona (26). Briefly, 32 L of raw skim milk was adjusted to 0.34 M NaCl and 1 mM phenylmethylsulfonyl fluoride (PMSF). Heparin-agarose (100 ml) was added successively to 8 L batches of milk and stirred for 45 min, after which the heparin-agarose-LpL was separated by filtration through a sintered glass filter. The lipoprotein lipase bound to the heparin-agarose was washed successively with buffer containing 10 mM Tris-HCl, 0.2% NaN_3 (pH 6.5), and either 0.5 M or 0.75 M NaCl. The washed material was packed into a column and further washed with buffer containing 10 mM Tris-HCl, 0.2% NaN_3, and 0.75 M NaCl, pH 6.4. The LpL was eluted from the agarose with a 1.0–2.0 M linear gradient of NaCl. All procedures were performed at 4°C. Samples were stored in 2 M NaCl at −20°C until required, and when thawed were stored at 4°C and used within a week. LpL samples were dialyzed for 24 h at 4°C against four changes of buffer containing 10 mM Tris-HCl, 0.15 M NaCl, 1 mM EDTA, 0.1% NaN_3, and 15 mM heparin, pH 7.4.

Analytical ultracentrifugation

Sedimentation velocity and equilibrium experiments were conducted with a Beckman XL-A analytical ultracentrifuge equipped with absorption optics, and using an An60-Ti rotor. Flotation coefficients (s_f) were calculated from the gradient of a plot of ln(r) versus $\omega^2 t$, where r is the radial distance to the midpoint of the solute boundary, t is the time at which the scan was taken, and ω is the radial velocity. Optical density data were acquired at radial increments of 0.005 cm, each data point being an average of five measurements. Storage of the emulsion fractions at 4°C over 7 days did not change the flotation coefficients.

Flotation velocity experiments were also analyzed to obtain the sedimentation (or flotation) distribution function (g(s*)), calculated from the time derivative of the concentration profile (27, 28). This method eliminates time independent factors such as baseline contributions and random noise. An additional advantage of the method is that it allows detection of multiple species such as those formed upon interaction of LpL with the emulsion particles. When diffusion is negligible, the apparent distribution function can be regarded as equivalent to the true distribution of flotation coefficients. Radial scans were taken at eight time points after the solute had left the bottom of the centrifuge cell. Scans were plotted on a 0.01 cm radial increment grid, and subtracted to give functions of $\Delta c/\Delta t$ (where $\Delta c/\Delta t \approx \delta c/\delta t$). These data were smoothed by three passes of a moving average using a window spanning 2% of the total data set. As this smoothing introduces artificial spreading into the g(s*) distribution functions, all data sets were smoothed to the same degree. Values of $\delta c/\delta t$ were converted to the weight fraction distribution function as described by Stafford (27, 28).

$$g(s^*) = \delta c(r,t)/\delta t \cdot (t/s^*) \cdot (1/c_0) \cdot (r/r_m)^2 \quad \textit{Eq. 1)}$$

where r_m is the radial position of the meniscus and c_0 is the initial solute concentration: r/r_m is the correction for the radial concentration. The g(s*) analysis was performed using the program Dc_Dt (28) modified for flotation as opposed to sedimentation.

The partial specific volumes ($\bar{v}$) of emulsion fractions were determined by flotation velocity experiments in H_2O and D_2O (29).

$$s_f(H_2O) = s_f(D_2O)\ (1 - \bar{v}\rho(H_2O))/(1 - \bar{v}\rho(D_2O)) \quad \textit{Eq. 2)}$$

where ρ is the solution density and the flotation coefficients, $s_f(H_2O)$ and $s_f(D_2O)$, refer to values determined experimentally using solutions containing either H_2O or a mixture of H_2O and D_2O, respectively.

Flotation equilibrium distributions were obtained at 20°C using an angular velocity of 1500 rpm. Absorbance data were obtained at radial increments of 0.001 cm, each data point being the average of 5 measurements. Cells were scanned at 240 nm every 4 h and the condition of equilibrium was assumed when successive scans showed no change in the concentration distribution. High speed depletion of the solute was performed at 20,000 rpm for 2 h to determine the baseline contribution. The equilibrium distributions obtained at multiple wavelengths were fitted assuming a single species using the program MULTEQ kindly provided by Dr. A. P. Minton, National Institutes of Health, Bethesda. Size heterogeneity of emulsion samples was assessed by comparison of number average with the weight-average molecular weights (30) according to Lechner and Mächtle (31) using a program kindly provided by Dr. M. D. Lechner, University of Osnabrueck, Germany.

RESULTS

Fractionation of emulsions

Emulsions composed of TO and DMPC were prepared by sonication and pressure extrusion and subjected to sucrose gradient centrifugation. The distribution of material was monitored for light scattering by measuring the absorbance at 250 nm (**Fig. 1A**) and for phospholipid and triacylglycerol content (Fig. 1B). The arrow in Fig. 1A indicates the predicted position in the density gradient of emulsion particles of radius 42 nm (see Materials and Methods). Material at the top of the

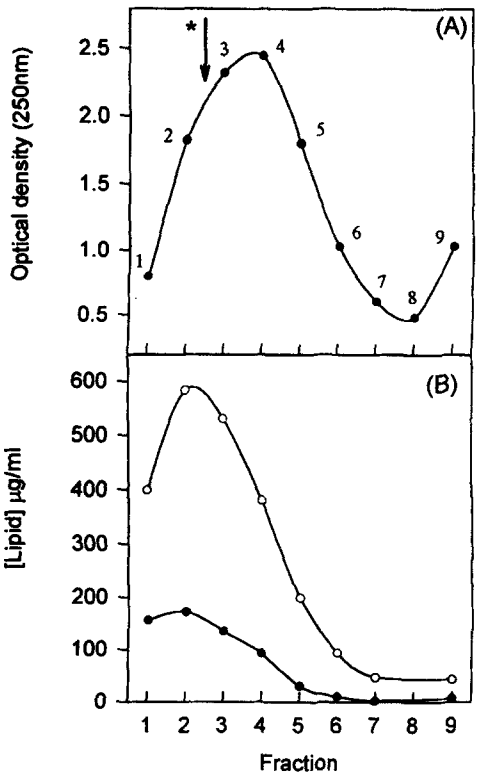

Fig. 1. A: Sucrose density gradient fractionation of lipid emulsions formed by extrusion through polycarbonate filters (see Materials and Methods). Fractions (1 ml) were collected from the bottom of the centrifuge tube. The arrow indicates the migration position predicted for a particle of $\bar{v}$ 1.09 ml/gm and radius 42 nm. B: Corresponding distributions of TO (○) and DMPC (●).

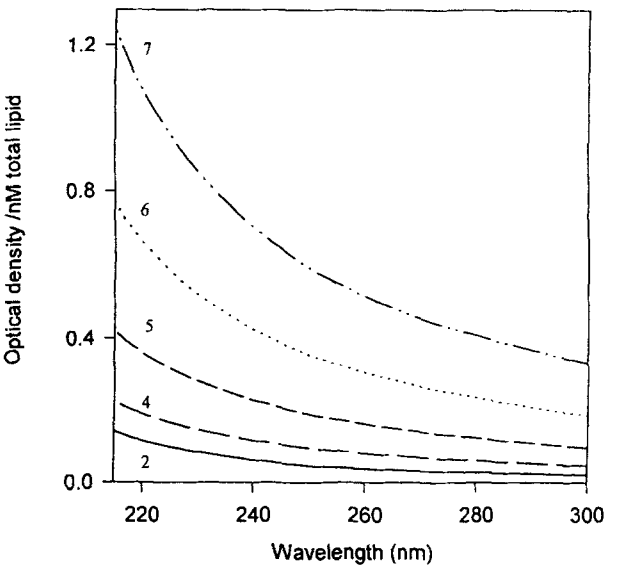

Fig. 2. Absorption spectra of emulsions fractionated by density gradient centrifugation. Spectra have been normalized to account for differences in lipid concentration. The numbers refer to the fractions shown in Fig. 1.

gradient (Fig. 1, fraction 9) was presumed to consist of aggregated lipid material and was not investigated further. The profiles obtained for different emulsion preparations were highly reproducible. The main peak in the light scattering profile (Fig. 1A) appears slightly in front (by 1–2 ml) of the peak in the triacylglycerol and phospholipid profiles shown in Fig. 1B. Thus, particles with faster rates of flotation scatter more light relative to their lipid content. This observation is confirmed by the data in **Fig. 2** where the wavelength-dependence of light scattering for each fraction is normalized against the total lipid content. These data were fitted to the Cashin-Debye equation to obtain the particle radii (24). Particle size was also determined from the TG:PC ratio assuming that each TG molecule occupies a volume of 1610 Å^3 (32) and that each phospholipid molecule occupies an area of 60 Å^2 and forms a surface monolayer that is 20 Å thick (18). Values of the average particle molecular weight were then calculated from the particle radii and the partial specific volumes of the TG and PC.

The results are summarized in **Table 1.** The TG:PC ratio decreases progressively from 7.60 in fraction 5 (top) to 2.78 in fraction 1 (bottom), indicating that the particles fractionate on the basis of their relative triacylglycerol and phospholipid contents. Larger particles containing a higher proportion of triacylglycerol have a faster flotation rate in the density gradient and therefore appear in the higher fractions. There is good agreement in the particle size whether determined from the light scattering data or on the basis of the TG:PC ratio. The radii (30–67 nm) correspond to particle molecular weights in the range 0.47×10^8 to 7.05×10^8. The

TABLE 1. Analysis of lipid emulsion fractions from sucrose gradient centrifugation

Fraction[a]	TG:PC	Radius[b]	$\bar{v}$[c]	Radius[d]	Mol. Wt.[e]
	molar ratio	*nm*	*ml/g*	*nm*	*$\times 10^{-8}$*
1	2.78	—	1.057	30	0.47
2	4.51	31	1.067	42	1.75
3	5.37	35	1.070	49	2.77
4	6.73	47	1.074	60	5.07
5	7.60	62	1.076	67	7.05

[a]Fractions from sucrose density gradient centrifugation of emulsions prepared by pressure extrusion (see Methods).

[b]Radii of the emulsion fractions determined from the wavelength dependence of scattered light in Fig. 2 (24).

[c]The weight average partial specific volume ($\bar{v}$) from the TG:PC ratio assuming values of $\bar{v}$ of 1.094 ml/g and 0.943 ml/g for TG and PC, respectively (42).

[d]Average particle radii were calculated from the TG:PC ratio assuming each PL molecule occupies an area of 60 Å^2 in the surface monolayer, and that each TG molecule occupies a volume of 1610 Å^3 in the particle core (14, 18).

[e]Determined from values of the particle radii[d] and $\bar{v}$.

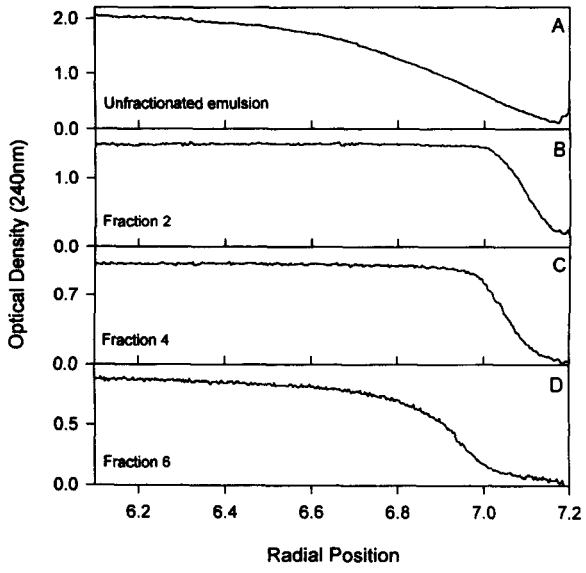

Fig. 3. Flotation velocity profiles of unfractionated and fractionated lipid emulsions. Samples contained 300 μg total lipid and centrifugation was at 3000 rpm and 20°C. Scans were taken at the same time (1.2 h) after the start of centrifugation.

TABLE 2. Flotation velocity analysis of lipid emulsion particles

Fraction[a]	$s_f(H_2O)$[b]	$s_f(D_2O)$[b]	$\bar{v}$[c]	Mol. Wt.[d]	Radius[e]
			ml/g	$\times 10^{-8}$	*nm*
1	112	190	1.055	0.52	28
2	299	361	1.063	2.08	44
3	404	—	—	3.24	51
4	651	—	—	5.77	62
5	760	1141	1.082	6.02	64
6	926	—	—	—	—
7	1124	—	—	—	—

[a]Fractions from sucrose density gradient centrifugation of emulsions prepared by pressure extrusion (see Materials and Methods).

[b]Flotation coefficients were calculated from the rate of movement of the solute boundary, corrected for density and viscosity effects of the buffer (see Materials and Methods). Flotation coefficients were determined using H_2O (density 1.011 mg/ml) or 50% D_2O (density 1.055 mg/ml) as the solvent. The effect of density on flotation behaviour was used to calculate the partial specific volume ($\bar{v}$) of the particles.

[c]Weight average partial specific volume determined according to equation 2.

[d,e]Average molecular weight and radii of the particles were calculated from the measured flotation coefficients and partial specific volumes, and assuming spherical symmetry. For fractions 1, 2, and 5, the values of $\bar{v}$ were those calculated according to equation 2. For fractions 3 and 4, the values of $\bar{v}$ were estimated from the TG:PC ratio (Table 1).

TG:PC ratios were not determined for fractions 6 and 7 (Fig. 1) due to their low lipid concentration.

Flotation velocity analysis of fractionated emulsions

The analytical ultracentrifuge was used to further characterize the fractions obtained by density gradient centrifugation. Absorbance profiles for unfractionated material and for three fractions from the density gradient (fractions 2, 4, and 6) obtained after centrifugation at 3000 rpm for 1.2 h are presented in **Fig. 3.** The flotation boundary for the unfractionated emulsion is broad, indicating significant size heterogeneity (Fig. 3A). By contrast, the boundaries obtained for the individual fractions are considerably sharper indicating greater size homogeneity. The flotation coefficients determined from the rate of movement of the midpoint of the solute boundary are summarized in **Table 2.**

A more complete analysis of the flotation velocity results was performed by g(s*) analysis (27). The flotation coefficient distribution for the unfractionated material is shown in **Fig. 4** and covers a wide range of flotation coefficients yielding an average value of 740 S. The distributions for the individual fractions are narrower, indicating greater size homogeneity. The flotation coefficients obtained from the position of the peak maximum for each fraction agree well with those obtained from the migration of the mid-point of the boundary (Table 2).

The possibility of association and/or fusion of emulsion particles was examined by centrifugation of a 1:1 (w/w total lipid) ratio of two distinct fractions. The g(s*) profiles obtained for such mixtures (**Fig. 5**) exhibited two peaks at positions that correspond to those of the individual fractions alone. The two populations of particles in the mixture therefore moved independently

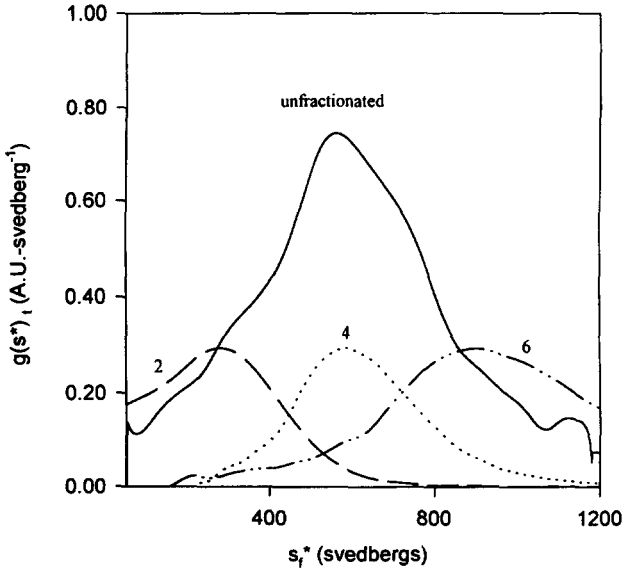

Fig. 4. Analysis of flotation velocity data for the unfractionated and fractionated lipid emulsion and using the time derivative of the concentration profile (27, 28) to obtain the apparent flotation distribution function (g(s*) vs. s_f). The numbers refer to the fractions collected in the density gradient experiment (Fig. 1).

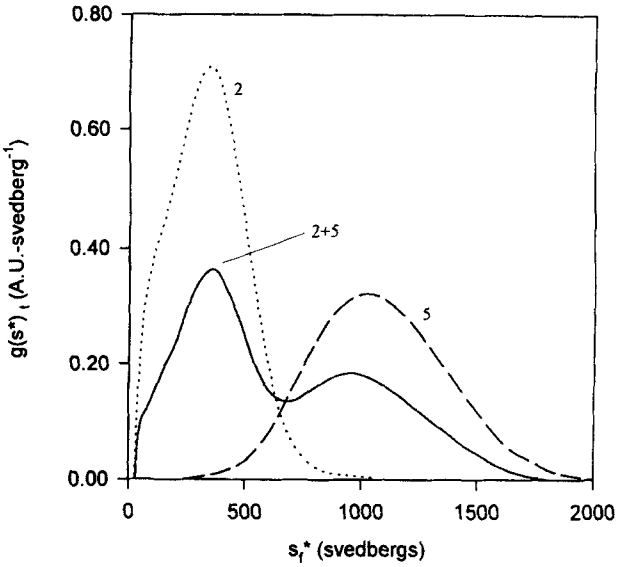

Fig. 5. Flotation velocity analysis of a 1:1 mixture of fractions 2 and 5 (2 + 5) compared with the individual fractions alone (2, 5). Total lipid concentration was 0.15 mg/ml for the individual fractions and for the mixture.

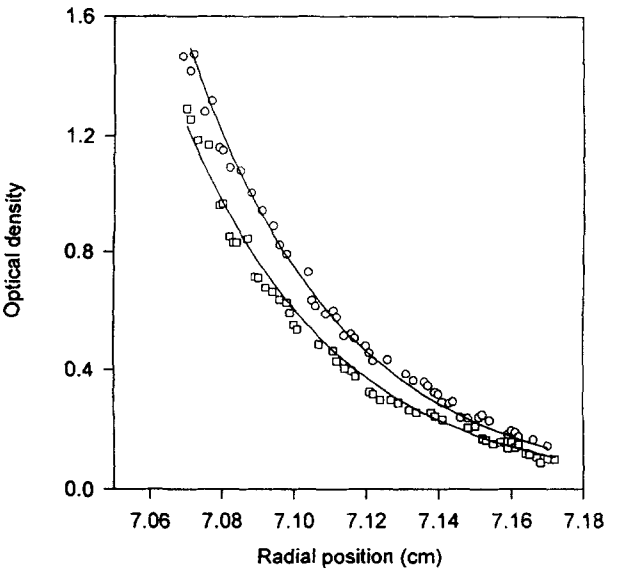

Fig. 6. Flotation equilibrium distributions for emulsion Fraction 1 (Fig. 1) measured at 235 nm (○) and 250 nm (□). Total lipid concentration was 0.1 mg/ml and centrifugation was at 1500 rpm for 26 h at 20°C. The solid lines are for the global fit of data collected at 235, 240, 245, and 250 nm.

of each other, with no measurable change occurring in the physical characteristics of the emulsion populations after mixing or during the course of the centrifuge run.

Interpretation of flotation coefficients in terms of particle size requires knowledge of the partial specific volume ($\bar{v}$) of the particle. Although estimates of $\bar{v}$ were obtained from the triacylglycerol and phospholipid content (Table 1), more precise values of $\bar{v}$ were obtained by performing flotation velocity experiments in H_2O and D_2O with subsequent application of equation 2 (29). The values of $\bar{v}$ for the emulsion particles in fractions 1, 2, and 5 are reported in Table 2. The results are in good agreement with those calculated from TG:PC ratios (Table 1). Assuming spherical symmetry, the molecular weight of the particles can be calculated from the measured flotation coefficients and values for the partial specific volume derived from flotation in H_2O and D_2O (fractions 1, 2, and 5; Table 2). Values of the particle radii (28–64 nm) and the particle molecular weights (0.52×10^8–6.02×10^8) agree well with those obtained by analysis of the TG:PC ratios (Table 1).

Flotation equilibrium analysis of emulsions

The flotation equilibrium technique offers an alternative approach for the characterization of emulsion size and heterogeneity. Its main advantage is that estimates of molecular weight can be made without the assumption of spherical symmetry. The lower limit to the angular velocities available with the Beckman XL-A ultracentrifuge (1500 rpm) restricted experiments to emulsions of small particle size. Representative equilibrium distributions obtained at 235 nm and 250 nm for fraction 1 are shown in **Fig. 6.** Profiles were also collected at 240 nm and 245 nm, and the complete data set was fitted globally assuming the presence of a single solute species. The value obtained for the reduced molecular weight, $M(1 - \bar{v}\rho)$, was -3.66×10^6. The value of $\bar{v}$ obtained for fraction 1 by analysis of the flotation velocity in H_2O and D_2O (1.055 ml/g, Table 2) provides a molecular weight of 0.55×10^8, a value in good agreement with that obtained by analysis of the flotation velocity coefficient (0.52×10^8, Table 2) and consideration of the TG:PC ratio (0.47×10^8, Table 1). Knowledge of the molecular weight, flotation coefficient and the $\bar{v}$ of the particles in fraction 1 allows calculation of the frictional ratio (f/f_0). The frictional ratio gives an indication of particle shape, the value of f/f_0 for a spherical molecule being unity. The f/f_0 value calculated for the emulsions in fraction 1 is 1.02 indicating that the particles are spherical, validating calculation of particle molecular weight made under the assumption of spherical symmetry (Table 2).

Evidence for the homogeneity of fraction 1 is provided by an analysis of the number-average (M_n) and weight-average (M_w) molecular weights (30). The ratio M_n/M_w of 1.13 obtained by analysis of the data at 240 nm is close to the value of unity expected for a single solute species. As scattered light varies with particle size

TABLE 3. Interaction of LpL with ether-linked lipid emulsions

Fraction[a]	LpL[b]	S_f (H_2O)	S_f (D_2O)	$\bar{v}$[d]	Mol. Wt.	Radius	LpL/particle[d]	PC/LpL[d]
	μM			*ml/g*	$\times 10^{-8}$	*nm*		
4	0	962	1218	1.085	6.98	67	—	—
5	0	1261	1540	1.086	9.80	75	—	—
7	0	1430	1620	1.088	11.5	79	—	—
4	2.8	698	965	1.055	7.63	68	1315 ± 70	71
5	2.8	958	1290	1.062	10.5	76	1449 ± 75	81
7	2.8	1180	1534	1.067	12.2	80	1466 ± 77	89

[a]Fractions from sucrose density gradient centrifugation of emulsions prepared by pressure extrusion (see Materials and Methods).

[b]The concentration of LpL was chosen to saturate the emulsion particles (Fig. 7). The total lipid concentration was 0.15 mg/ml.

[c]Flotation coefficients were calculated from the maximum in the flotation coefficient distribution function (Fig. 7) and corrected for density and viscosity effects of the buffer (see Materials and Methods). Flotation coefficients were determined using H_2O (density 1.008 mg/ml) or 25–30% D_2O as the solvent.

[d]The partial specific volume ($\bar{v}$) was estimated from the flotation coefficients determined in the D_2O or H_2O solvents and used to calculate the molecular weight and particle radii. The number of LpL monomers bound to the emulsion particle was calculated assuming a $\bar{v}$ and molecular weight for the protein of 0.726 ml/g and 48,300, respectively. The ratio of PC molecules in the surface monolayer per bound LpL was calculated assuming each PC molecule occupies an area of 60 $Å^2$ in a 20 Å thick monolayer.

(Fig. 1), the observation that data sets collected at several wavelengths can be globally fitted to a single molecular weight species provides additional support for the existence of an essentially homogeneous solute.

Interaction of LpL with non-hydrolyzable lipid emulsions

Lipid emulsions composed of non-hydrolyzable ether-linked phospholipid and triacylglycerol analogues were prepared and fractionated by sucrose gradient centrifugation. The density gradient profiles were similar to those reported in Fig. 1 for the ester-linked lipid emulsions. Determination of flotation coefficients and partial specific volumes permitted the molecular weights and radii of the fractionated ether-linked particles to be determined (**Table 3**).

The effect of LpL on the flotation behavior of ether-linked emulsions was explored by g(s*) analysis (**Fig. 7**). In the absence of LpL, the flotation coefficient distribution for emulsion fraction 4 was relatively symmetrical, with the peak corresponding to a flotation coefficient of 962 S (Fig. 7, curve a). The addition of a low concentration of LpL (0.35 μM) generated a more heterogeneous distribution leading to the appearance of species with higher flotation coefficients (1490 S) (Fig. 7, curve b). Additionally, considerable optically dense material floated rapidly to the top of the solution column prior to the collection of radial scans. This particle aggregation is interpreted as LpL-induced cross-linking, in accord with previous descriptions of the interactions between LpL and phospholipid vesicles (33). At higher concentrations of LpL, the predominant species moved at a rate slower than that of the emulsion alone. In the presence of 1.4 μM and 2.8 μM LpL, the flotation coefficient distributions were similar with peaks at approximately 700 S (Fig. 7, curves d and e). The changes observed in the flotation coefficient distributions on the addition of LpL indicate that binding of the enzyme to the emulsion particles occurs with saturation in the region of 1.4–2.8 μM LpL. Further evidence of saturation of the emulsion particles by LpL at the higher LpL

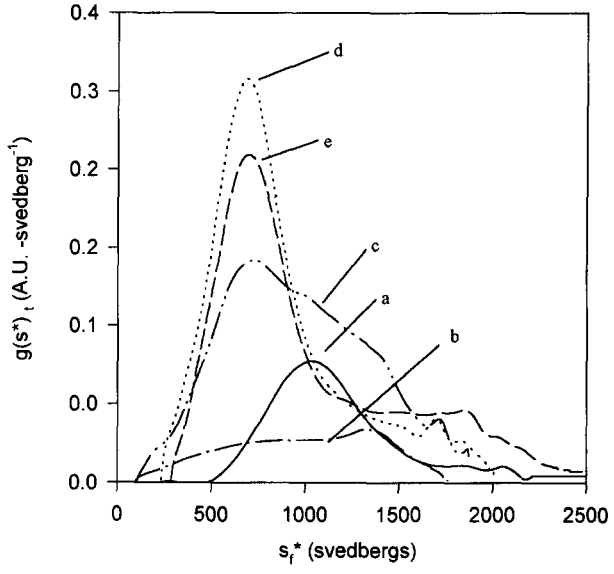

Fig. 7. Flotation velocity analysis of mixtures of LpL with non-hydrolyzable lipid emulsions. Samples (0.15 mg/ml total lipid) were prepared in 10 mM Tris-HCl, 0.15 M NaCl, 1 mM EDTA, pH 7.4) and centrifuged at 3000 rpm at 20°C). Scans were taken at 230 nm every 8 min. The flotation distribution profiles refer to LpL concentrations: a, 0; b, 0.35; c, 0.7; d, 1.4; and e, 2.8 μM.

levels is provided by the increased optical density in the infranatent region which is attributed to unbound LpL (results not shown).

Capacity of emulsions to bind LpL

Studies on the binding of LpL to ether-linked emulsions were also performed for fractions 5 and 7. The flotation velocity coefficients of emulsion particles saturated with LpL were determined in D_2O and H_2O, thereby allowing calculation of partial specific volumes, molecular weights and radii of the protein–lipid complexes. The results summarized in Table 3 show that as the flotation coefficient of the original emulsion particles increases, the $\bar{v}$ of the LpL-saturated particle also increases. Values of the partial specific volume of the protein (0.726 ml/g, (34)), the emulsion alone, and the emulsion–LpL complex (Table 3) were used to calculate the amount of protein bound to each particle. The results presented in Table 3 indicate that there are 1315–1466 molecules of LpL per lipid particle, corresponding to PC:LpL ratios ranging from 71 (for the smaller particles) to 89 (for the larger particles). The increases in the molecular weights of the emulsion particles on binding LpL (Table 3) were close to those calculated from the numbers of molecules of bound LpL.

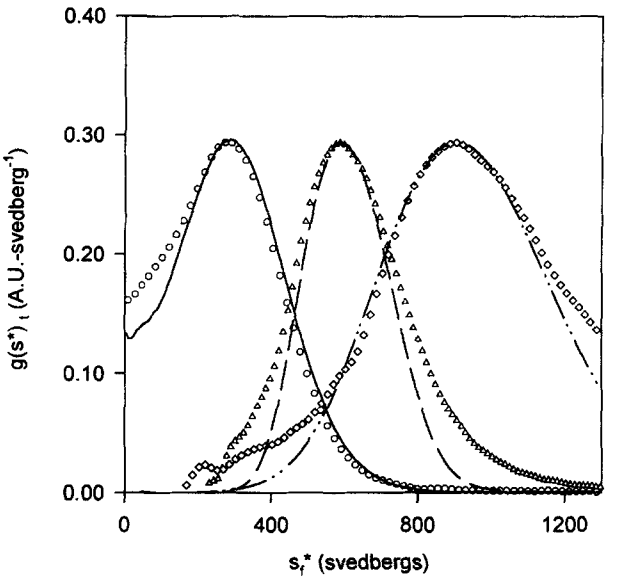

Fig. 8. Simulation of flotation velocity data of ideal homogeneous solutes. Values used in the simulation correspond to the flotation coefficients reported in Table 2 for fractions 2, 4, and 6 and diffusion coefficients calculated assuming spherical particles. Data describing s_f 299 S, D = 0.48×10^{-7} cm^{2}sec^{-1} (solid line), s_f 651 S, D = 0.31×10^{-7} cm^{2}sec^{-1} (dashed line), and s_f 926 S, D = 0.29×10^{-7} cm^{2}sec^{-1} (dashed, dotted line) were simulated using the program SIMCENT and are compared to the experimental data for fractions 2 (circles), 4 (triangles), and 6 (diamonds). Every 10th experimental data point has been plotted, for clarity.

DISCUSSION

Heterogeneity in the size and composition of lipid emulsions is a major impediment to their use as model systems for physicochemical investigations of protein–lipid interactions of relevance to lipoprotein chemistry. Previous studies have demonstrated that sonication of triolein/phosphatidylcholine suspensions produces emulsion particles with radii ranging from 50 to 250 nm (19). Repeated extrusion of these particles through polycarbonate filters of defined pore size yields more homogeneous particles of average radii 71 ± 18 nm (14) and in the size range of large VLDL particles. However, as is evident from the extremely diffuse flotation boundary in Fig. 3A, emulsions prepared by pressure extrusion remain heterogeneous. The sucrose density gradient procedure described here (Fig. 1) fractionates these preparations to provide material suitable for quantitative analysis using the analytical ultracentrifuge. Light scattering, TG:PC composition, and flotation velocity data (Tables 1, 2, and 3) establish the success of the fractionation technique, yielding estimates of particle radii for sequential fractions ranging from 28 to 79 nm. These methods for determining particle size assume a spherical shape, an assumption supported by flotation equilibrium analysis (Fig. 6) where the value for the weight average molecular weight (fraction 1, 0.57×10^8) from flotation equilibrium analysis is in excellent agreement with the value obtained from the flotation velocity measurements (Table 2).

The flotation distribution function g(s*) can potentially be used to access the residual polydispersity of the various fractions. In the absence of diffusion, the distribution function describes the distribution of sedimentation coefficients within the sedimenting population (27). However, theoretical calculations using diffusion coefficients appropriate for spherical particles of the molecular weights, partial specific volumes, and sedimentation coefficients described in Tables 2 and 3 indicate that diffusion is not negligible, particularly at the slow rotor speeds required to monitor the sedimentation boundary. The data in **Fig. 8** compare the theoretical behavior of ideal, homogeneous particles of the size reported for fractions 2, 4, and 6 (Tables 2 and 3) to the experimental data presented in Fig. 4. The results indicate that a significant amount of the spreading can be attributed to diffusion. Spreading can also be attributed to the finite time required to spectrophotometrically scan the centrifuge cell (typically 4–6 min). Thus, while g(s*) analysis indicates that the individual fractions are more homogeneous than the unfractionated

material (Fig. 4) and that mixed fractions of emulsions sediment independently (Fig. 5), it is difficult to specify the residual heterogeneity. A more rigorous measure of the heterogeneity is obtained from the flotation equilibrium experiments where the ratio of M_n/M_w of 1.13 and the fit of the experimental data to a single species (Fig. 6) indicate a high degree of homogeneity.

The scattering of light by large emulsion particles is a disadvantage when spectroscopic methods such as fluorescence and circular dichroism are used to study their interactions with proteins such as LpL. However, this scattering can be used to advantage to monitor such interactions in the analytical ultracentrifuge. The results in Fig. 7 show that flotation rates of non-hydrolyzable lipid emulsions, at low LpL/lipid ratios, are increased compared to the rate for emulsions alone. We interpret this as a direct consequence of the dimeric structure of LpL (3) leading to crosslinking of emulsion particles. It is likely that this crosslinking of particles by lipoprotein lipase is due to a cooperative event involving multiple dimers for each pair of crosslinked emulsion particles. This ability of the two LpL binding sites to interact with separate emulsion particles suggests that the sites are situated on opposite sides of the dimeric complex. Crosslinking by LpL dimers has been postulated as the mechanism for a non-enzymatic role of LpL where LpL dimers bind cholesterol-rich lipoproteins and lipoprotein remnants and mediate cellular uptake and degradation via interaction with specific protein receptors on the cell surface (8).

The flotation rate of emulsions saturated with LpL is reduced relative to emulsions alone (Fig. 7). This reduction is a direct result of the higher density of protein compared to the lipid emulsion. As the densities of the complex and the emulsions are close to that of the solvent, comparison of flotation rates in H_2O and H_2O/D_2O solvent mixtures provides a very sensitive measure of the amount of bound LpL. Analysis of the results in terms of partial specific volumes and molecular weights indicates emulsion particles in the size range 67–79 nm bind approximately one LpL monomer per 80 phospholipid molecules (Table 3) or 5.3 amino acids per phospholipid, based on a molecular weight for LpL of 48,300 (3). These results can be compared to previous studies on the binding of apolipoproteins A-I, A-II, C-II, and C-III to lipid emulsions where the binding capacities range from 0.3 to 1.3 amino acids per phospholipid (19). The higher binding capacity for LpL (per amino acid) may reflect the larger size of LpL or possibly the oligomeric state with only one active site of the dimer bound to the lipid surface. The experiments described in Table 3 indicate very little unbound LpL present in the infranatant region at subsaturating levels of LpL (0.3–0.7 μM) implying that at these concentrations most of the LpL is bound. While it is difficult to estimate the binding constant, the results suggest dissociation constants in the μM range and comparable to those reported previously for the binding of apolipoproteins (19).

The binding of LpL to unilamellar bilayer vesicles composed of non-hydrolyzable phospholipids (12–15 nm) has been studied by McLean and Jackson (20). Each LpL binding site was made up of 270–320 phospholipids, a figure substantially higher than those reported here (71–89 PC/LpL). Surface curvature effects may play an important role in determining the packing of LpL on the lipid surface. It has been suggested that there is a decrease in the interchain interactions of phospholipid molecules in lipid bilayers of increasing surface curvature (particle radii <50 nm (35, 26)). It is possible that an increase in surface curvature and a decrease in interchain interactions decreases the packing density of phospholipid head groups on the vesicle surface leading to reduced capacity to bind LpL.

The question arises as to how this capacity is related to the footprint and packing of LpL molecules on the emulsion surface. On the basis of its molar volume, the area projected by an LpL monomer onto the lipid surface is approximately 470 $Å^2$. Assuming hexagonal packing, an average particle of 74 nm radius could accept 1464 LpL monomers, a figure that is close to that determined experimentally (≈1410 ± 74). According to these calculations a high proportion of the surface of the emulsion (>90%) is covered by LpL at saturation, although this estimate could be significantly less if LpL is bound as dimers or higher oligomers. Lack of any observable phospholipid vesicles in the infranatant region during centrifugation indicates that the binding of LpL is not accompanied by a significant loss of lipid from the emulsion surface. Further evidence that LpL binding occurs without significant alteration in lipid composition is provided by the observation that the molecular weight of the LpL–emulsion complex (Table 3) is similar to that calculated from the molecular weight of the emulsion and the number of molecules of bound LpL.

An important question is whether LpL binds to the surface of the emulsion particle thereby accessing the sparingly soluble triacylglycerols (2–4 mol %) present in the phospholipid monolayer, or whether LpL penetrates the surface with resultant disruption of phospholipid order. McLean, Larsen, and Jackson (33) observed little change in the structure or motion of a lipid bilayer upon addition of saturating concentrations of LpL. Penetration of the emulsion surface by the protein is presumed to depend on the surface pressure of the phospholipid. Generally, proteins cannot penetrate a phospholipid monolayer at surface pressures greater

than 30 mN/m (for review, see ref. 37), and it is known that LpL and hepatic lipase have negligible activity at surface pressures greater than 30 mN/m (11, 38). The surface pressure within the emulsion surface is not known. However, substantial movement of LpL into the surface monolayer would displace phospholipids which would then form separate vesicle–LpL complexes. As indicated above, no such complexes were evident in the flotation velocity experiments, suggesting that LpL does not penetrate the surface monolayer of ether-linked phospholipids to a significant degree. Penetration of the surface monolayer may occur in the subsequent steps of the interaction of LpL with ester-linked lipid emulsions where lipid hydrolysis can remove surface lipids and reduce the surface pressure.

A number of studies have examined the LpL-catalyzed hydrolysis of triacylglycerols isolated as native lipoproteins from human plasma (17, 39–41). Such studies of the activity of LpL towards native substrates are hampered by uncertainties surrounding the composition of the particles. For example, Connelly et al. (17) reported different values for the K_m of LpL for small native VLDL particles compared to large particles, but similar values for V_{max}, in contrast to results obtained with synthetic substrates (16). The interpretation of results derived from native particles is complicated by the need to consider variation in lipid and apolipoprotein composition both between and within lipoprotein populations. This is particularly true for quantitation of the level of apoC-II, an in vivo activator of LpL. Procedures to fractionate lipid emulsions of different size and composition, as described in the present work, will facilitate studies on the substrate specificity and cofactor requirements of LpL-catalyzed lipid hydrolysis.

We thank Dr. Simon Easterbrook-Smith for help with the light scattering analysis and Mr. Graham Grieve for help with the triacylglycerol determinations. This work was supported by grants to WHS and GJH from the Australian National Health and Medical Research Council. CEM is the recipient of an Australian Postgraduate Research Award.

Manuscript received 25 November 1996, in revised form 25 February 1997, and in re-revised form 5 May 1997.

REFERENCES

1. Wang, C-S., J. Hartsuck, and W. J. McConathy. 1992. Structure and functional properties of lipoprotein lipase. *Biochim. Biophys. Acta.* **1123:** 1–17.
2. Atkinson, D., and D. M. Small. 1986. Recombinant lipoproteins: implications for structure and assembly of native lipoproteins. *Annu. Rev. Biophys. Chem.* **15:** 403–456.
3. Osborne, J. C., G. Bengtsson-Olivecrona, N. S. Lee, and T. Olivecrona. 1985. Studies on inactivation of lipoprotein lipase: role of the dimer to monomer dissociation. *Biochemistry.* **24:** 5606–5611.
4. Olivecrona, T., and G. Bengtsson-Olivecrona. 1987. Lipoprotein lipase from milk: the model enzyme in lipoprotein lipase research. *In* Lipoprotein Lipase. J. Borensztajn, editor. Evener, Chicago. 15–59.
5. Vilella, E., J. Joven, M. Fernandez, S. Vilaro, J. D. Brunzell, T. Olivecrona, and G. Bengtsson-Olivecrona. 1993. Lipoprotein lipase in human plasma is mainly inactive and associated with cholesterol-rich lipoproteins. *J. Lipid Res.* **34:** 1555–1564.
6. Williams, S. E., I. Inoue, H. Tran, G. L. Fry, M. W. Pladet, P-H. Iverius, J-M. Lalouel, D.A. Chappell, and D. K. Strickland. 1994. The carboxyl-terminal domain of lipoprotein lipase binds to the low density lipoprotein receptor-related protein/α_2-macroglobulin receptor (LRP) and mediates binding of normal very low density lipoproteins to LRP. *J. Biol. Chem.* **269:** 8653–8658.
7. Chappell, D. A., I. Inoue, G. L. Fry, M. W. Pladet, S. L. Bowen, P-H. Iverius, J-M. Lalouel, and D. K. Strickland. 1994. Cellular catabolism of normal very low density lipoproteins via the low density lipoprotein receptor-related protein/α_2-macroglobulin receptor is induced by the C-terminal domain of lipoprotein lipase. *J. Biol. Chem.* **269:** 18001–18006.
8. Nykjær, A., M. Nielsen, A. Lookene, N. Meyer, H. Røigaard, M. Etzerodt, U. Beisiegel, G. Olivecrona, and J. Gliemann. 1994. A carboxyl-terminal fragment of lipoprotein lipase binds to the low density lipoprotein receptor-related protein and inhibits lipase-mediated uptake of lipoprotein in cells. *J. Biol. Chem.* **269:** 31747–31755.
9. Deckelbaum, R. J., J. A. Hamilton, A. Moser, G. Bengtsson-Olivecrona, E. Butbul, Y. A. Carpentier, A. Gutman, and T. Olivecrona. 1990. Medium-chain versus long-chain triacylglycerol hydrolysis by lipoprotein lipase and hepatic lipase: implications for the mechanism of lipase action. *Biochemistry.* **29:** 1136–1142.
10. Demel, R. A., P. J. Dings, and R. L. Jackson. 1984. Effect of monolayer lipid structure and composition on the lipoprotein lipase-catalyzed hydrolysis of triacylglycerol. *Biochim. Biophys. Acta.* **793:** 399–407.
11. Jackson, R. L., E. Ponce, and L. R. McLean. 1986. Comparison of the triacylglycerol hydrolase activity of human post-heparin plasma lipoprotein lipase and hepatic triacylglycerol lipase. A monolayer study. *Biochemistry.* **25:** 1166–1170.
12. Ginsburg, G. S., D. M. Small, and D. Atkinson. 1982. Microemulsions of phospholipids and cholesterol esters. *J. Biol. Chem.* **257:** 8216–8227.
13. Reisinger, R. E., and D. Atkinson. 1990. Phospholipid/cholesteryl ester microemulsions containing unesterified cholesterol: model systems for low density lipoproteins. *J. Lipid Res.* **31:** 849–858.
14. Drew, J., A. Liodakis, R. Chan, H. Du, M. Sadek, R. Brownlee, and W. H. Sawyer. 1990. Preparation of lipid emulsions by pressure extrusion. *Biochem. Int.* **22:** 983–992.
15. Li, Q-T., and W. H. Sawyer. 1992. Effect of cholesteryl ester on the distribution of fluorescent cholesterol analogues in triacylglycerol-rich emulsions. *J. Lipid Res.* **33:** 503–512.
16. Tajima, S., S. Yokoyama, and A. Yamamoto. 1984. Mechanism of action of lipoprotein lipase on triolein particles: effect of apolipoprotein C-II. *J. Biochem.* **96:** 1753–1767.
17. Connelly, P. W., G. F. Maguire, C. Vezina, R. A. Hegele, and A. Kuksis. 1994. Kinetics of lipolysis of very low density lipoproteins by lipoprotein lipase. *J. Biol. Chem.* **269:** 20554–20560.

18. Miller, K. W., and D. M. Small. 1983. Triolein–cholesterol oleate–cholesterol–lecithin emulsions: structural models of triglyceride-rich lipoproteins. *Biochemistry.* **22:** 443–451.
19. Tajima, S., S. Yokoyama, and A. Yamamoto. 1983. Effect of lipid particle size on association of apolipoproteins with lipid. *J. Biol. Chem.* **258:** 10073–10082.
20. McLean, L. R., and R. L. Jackson. 1985. Interaction of lipoprotein lipase and apolipoprotein C-II with sonicated vesicles of 1,2-ditetradecylphosphatidylcholine: comparison of binding constants. *Biochemistry.* **24:** 4196–4201.
21. McKeone, B. J., H. J. Pownall, and J. B. Massey. 1986. Ether phosphatidylcholines: comparison of miscibility with ester phosphatidylcholines and sphingomyelin, vesicle fusion, and association with apolipoprotein A-I. *Biochemistry.* **25:** 7711–7716.
22. Halperin, G., O. Stein, and Y. Stein. 1986. Synthesis of ether analogs of lipoprotein lipids and their biological applications. *Methods Enzymol.* **129:** 816–848.
23. Kates, M. 1972. Techniques of Lipidology: Isolation, Analysis and Identification of Lipids. T. S. Work and E. Work, editors. American Elsevier Publishing Co., New York.
24. Easterbrook-Smith, S. 1993. A light-scattering method for measuring the size of insoluble immune complexes. *Molec. Immunol.* **30:** 637–640.
25. Debye, P., and W. M. Cashin. 1949. Determination of molecular weight and sizes by absorption. *Phys. Rev.* **52:** 1307.
26. Bengtsson-Olivecrona, G., and T. Olivecrona. 1991. Phospholipase activity of milk lipoprotein lipase. *Methods Enzymol.* **197:** 345–356.
27. Stafford, W. F. 1992. Boundary analysis in sedimentation transport experiments: a procedure for obtaining sedimentation coefficient distributions using the time derivative of the concentration profile. *Anal. Biochem.* **203:** 295–301.
28. Stafford, W. F. 1994. Boundary analysis in sedimentation velocity experiments. *Methods Enzymol.* **240:** 478–501.
29. Edelstein, S. J., and H. K. Schachman. 1967. The simultaneous determination of partial specific volumes and molecular weights with microgram quantities. *J. Biol. Chem.* **242:** 306–311.
30. Yphantis, D. A. 1964. Equilibrium ultracentrifugation of dilute solutions. *Biochemistry.* **3:** 297–317.
31. Lechner, M. D., and W. Mächtle. 1992. Sedimentation equilibrium measurements with the new analytical ultracentrifuge Optima XL-A and its digital ultraviolet/visible detector. *Makromol. Chem.* **13:** 555–563.
32. Singleton, W. S. 1960. Fatty Acids. K. S. Markley, editor. 2nd ed. Part I. Interscience, New York. 499.
33. McLean, L. R., W. J. Larsen, and R. L. Jackson. 1986. Interaction of lipoproteins lipase with phospholipid vesicles: effect on protein and lipid structure. *Biochemistry.* **25:** 873–878.
34. Iverius, P. H., and A. M. Östlund-Linqvist. 1976. Lipoprotein lipase from bovine milk: isolation procedure, chemical characterization, and molecular weight analysis. *J. Biol. Chem.* **251:** 7791–7795.
35. Lichtenberg, D., E. Freire, C. F. Schmidt, Y. Barenholz, P. L. Felgner, and T. E. Thompson. 1981. Effect of surface curvature on stability, thermodynamic behaviour, and osmotic activity of dipalmitoylphosphatidylcholine single lamellar vesicles. *Biochemistry.* **20:** 3462–3467.
36. Parmar, Y. I., S. R. Wassall, and R. J. Cushley. 1984. Orientational order of phospholipid bilayers. ^{2}H NMR study of selectively deuterated palmitic acids in unilamellar vesicles. *J. Am. Chem. Soc.* **106:** 2434–2435.
37. Verger, R., and F. Pattus. 1982. Lipid–protein interactions in monolayers. *Chem. Phys. Lipids.* **30:** 189–227.
38. Laboda, H. M., J. M. Glick, and M. C. Phillips. 1988. Influence of the structure of the lipid–water interface on the activity of hepatic lipase. *Biochemistry.* **27:** 2313–2319.
39. Musliner, T. A., P. N. Herbert, and M. J. Kingston. 1979. Lipoprotein substrates of lipoprotein lipase and hepatic triacylglycerol lipase from human post-heparin plasma. *Biochim. Biophys. Acta.* **575:** 277–288.
40. Saheki, S., I. Takahashi, M. Murase, N. Takeuchi, and K. Uchida. 1991. Composition of very low density lipoproteins and in vitro effect of lipoprotein lipase. *Clin. Chim. Acta.* **204:** 155–166.
41. Gomez-Coronado, D., G. T. Saez, M. A. Lasuncion, and E. Herrera. 1993. Different hydrolytic efficiencies of adipose tissue lipoprotein lipase on very low density lipoprotein subfractions separated by heparin-Sepharose chromatography. *Biochim. Biophys. Acta.* **1167:** 70–78.
42. Small, D. M. 1986. Handbook of Lipid Research: The Physical Chemistry of Lipids. D. J. Hanahan, editor. Plenum Press, New York.